# Saharan and Namib Dust Phosphorus Fluxes in the North and South **Atlantic Regions**

Published as part of ACS Earth and Space Chemistry special issue "Hartmut Herrmann Festschrift".

Khanneh W. Fomba,\* Daniel T. Quaye, Eric P. Achterberg, Eugene Marais, and Hartmut Herrmann\*



Downloaded via HELMHOLTZ ZENTRUM OCEANFORSCHUNG on June 20, 2025 at 08:32:25 (UTC) See https://pubs.acs.org/sharingguidelines for options on how to legitimately share published articles.

Cite This: ACS Earth Space Chem. 2025, 9, 1465-1478



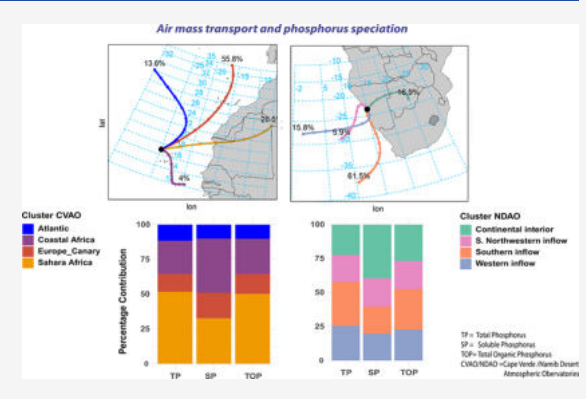
**ACCESS** I

Metrics & More

Article Recommendations

Supporting Information

ABSTRACT: Phosphorus (P) is essential for marine ecosystems, particularly in nutrient-poor regions of the Northeastern and Southeastern Tropical Atlantic (NETA/SETA). However, P deposition and bioavailability remain poorly understood, limiting predictions of its role in marine productivity. To address this, P speciation, including organic, inorganic, and soluble contents in aerosol particles, was analyzed over 19 months at the Cape Verde (CVAO) and Namib Desert (NDAO) Atmospheric Observatories. P concentrations at NDAO (56.1  $\pm$  62 ng/m<sup>3</sup>) were 47% higher than those at CVAO (29.8  $\pm$  76 ng/m<sup>3</sup>) with dominant coarse mode contents and fine-to-coarse ratios (PM<sub>1,2</sub>/PM<sub>10</sub>) of 0.42-0.57 at NDAO and 0.17–0.32 at CVAO. Phosphorus sources at both sites include mineral dust and biomass burning with additional biogenic aerosols at NDAO. Organic P made up 19% and 39% of total P at NDAO and CVAO,



respectively. Soluble P was 20% more abundant at NDAO, linked to higher biomass burning source provenance and aerosol acidity, confirming previous reports that atmospheric processing enhances P solubility. P solubility was lower during Saharan and Namib dust events, indicating comparatively reduced solubility from mineral-dust sources. This first report of annual deposition fluxes from these regions reveals somewhat higher average values in the SETA (2.05  $\pm$  2.8  $\mu$ mol/m<sup>2</sup>d at NDAO) than the NETA (1.3  $\pm$  3.4 μmol/m<sup>2</sup>d at CVAO), with pronounced differences in the austral winter months. Elevated dissolved inorganic nitrogen to dissolved inorganic P ratios at CVAO indicated a smaller contribution of atmospheric P deposition in mitigating nutrient limitation in the nearby waters. These findings offer new insights into atmospheric P solubility and fluxes, crucial for improving ocean-atmosphere models and understanding its ecological impacts in the tropical Atlantic.

KEYWORDS: phosphorus speciation, phosphorus solubility, atmospheric processing, Saharan dust, ocean fertilization, Benguela marine ecosystem

### 1. INTRODUCTION

Phosphorus (P) is an essential element for all living organisms and plays a critical role in primary production in marine ecosystems. 1-4 P is a critical component of plant and phytoplankton structure and function, contributing to processes such as protein synthesis, lipid metabolism, and sugar storage associated with primary production. P availability also influences species distribution and ecosystem structure, carbon sequestration, the carbon cycle, and the biological carbon pump. 3,6-8 However, P concentrations in surface waters and other marine ecosystems can be lower than the classical Redfield stoichiometric ratios required for optimum marine productivity, leading to reduced primary production rates due to phytoplankton growth limitation or colimitation<sup>9,10</sup> and shifts in species composition and diversity within phytoplankton communities.<sup>11</sup>

Ambient aerosol P can be sourced from soil-suspended dust particles containing P minerals, including apatite, both

hydroxyapatite [Ca<sub>5</sub>(PO<sub>4</sub>)<sub>3</sub>(OH)] and fluorapatite  $[Ca_5(PO_4)_3(F), FAP]$ , volcanic ash, and anthropogenic sources of mineral fertilizer. It also originates from biogenic particles, P manufacturing plants, and combustion processes, including biomass burning. 12-14 These aerosol particles are often a combination of inorganic (such as iron/calciumbounded P) and organic P (such as diesters and monoesters or plant-containing P complexes) that are present in both fine (<1  $\mu$ m) and coarse (>1  $\mu$ m) particle fractions depending on the emission processes. 5,15 Their transport to different regions

Received: December 30, 2024 Revised: May 22, 2025 Accepted: May 22, 2025

Published: June 10, 2025





subsequently affects local P budgets in terrestrial ecosystems but also plays an important role in fertilizing the ocean.

P in the ocean primarily originates from river inputs through weathering of rocks and minerals, anoxic shelf sediments, and atmospheric deposition. <sup>2,3,16–19</sup> While river inputs are significant along coastal continental margins, atmospheric deposition and anoxic shelf sediments in oxygen minimum zones are important P sources for open ocean ecosystems. Studies have reported P colimitations in surface waters in the North Atlantic and Red Sea. <sup>2,18,20</sup> Additionally, P concentrations in surface waters have shown strong correlations with atmospheric inputs in the Mediterranean Sea, where atmospheric deposition accounts for a significant increase in primary productivity. <sup>21–23</sup> Studies in the Baltic Sea have highlighted its practical importance alongside riverine inputs by emphasizing the underestimation of atmospheric P deposition in models. <sup>24</sup>

Although the total P mass is important in terms of supply, it is not the decisive biogeochemical parameter that is essential for marine and terrestrial ecosystems, but rather the bioavailable fraction that can be readily taken up by the metabolisms of organisms. P bioavailability is thought to be dependent on its solubility, with orthophosphate often considered the most soluble form of P. 25 Although mineral dust is a significant source, other sources also provide soluble content, 12,26,27 with combustion-related aerosol, in particular, revealing higher soluble contents. 12 In addition, the condensation of acidic species on surfaces containing P particles leads to interactions that modify the solubility of P particles and are dependent on particle size with smaller particles having a larger surface-to-volume ratio. Currently, the role of these interactions in the atmospheric processing of P-containing aerosol particles is still not well understood, with various parametrizations being tested and implemented in models for more accurate predictions of solubility, 28,29 making it difficult to predict the fate and impact of atmospheric P deposition. <sup>30,31</sup>

As apatite minerals are the main source of P, with low photo reactivity, and as Ca does not strongly bond with organic ligands, Stockdale et al.<sup>32</sup> highlighted that acid processing of aerosols that largely consist of dust particles is the most dominant process that increases soluble P fraction. They found that acid dissolution is controlled by proton ion concentration, with low proton ion to dust ratio ( $\hat{H}^+ < 10^{-4} \text{ mol/g of dust}$ ) already able to dissolve 1-10% of the total P that is surfacebound and higher ratios resulting in even higher P release. Although calcite may reduce the P dissolution due to acid buffering, this did not significantly affect the dissolution of apatite-P minerals dominant in dust particles.<sup>32</sup> Applying a simple relationship between atmospheric acidity and bioavailable P forms, Herbert et al.<sup>23</sup> showed that acid processing of aerosol particles may be important for P availability in the Mediterranean Sea and the Northeast Atlantic Ocean.

In the Northeastern and Southeastern Tropical Atlantic (NETA and SETA) Ocean regions, significant amounts of different types of mineral dust with varying P content (0.02 Tg/yr, North Atlantic; 0.005 Tg/yr, South Atlantic) are annually deposited into surface waters from nearby deserts. However, our understanding of this process is limited due to a lack of available data. Previous studies that quantified the temporal variability of P budgets in these regions were based on short-term campaigns, thus providing snapshots of concentrations dominated by abrupt emissions, but unable to characterize long-term fluxes and sources. <sup>33,34</sup> To bridge this

knowledge gap, we focused on targeted sampling at two locations: (i) the Cape Verde Islands, representative of continental inputs into the NETA from West and North Africa, including Saharan dust, and (ii) a near coastal location in Namibia, representative of P inputs into the SETA of Namib Desert dust and particulate matter (PM) from industries and biomass burning in the southern African interior. Although these are specific sampling locations, these sites provide valuable insights into the dynamics of nutrient and P source variations and subsequent fluxes into the oceans.

The primary objectives of this work are to provide a comprehensive data set on the concentrations, size distributions, solubility, and speciation of atmospheric P inputs to the NETA and SETA regions. In particular, the factors controlling the speciation of soluble and total P for these regions, as well as the role of atmospheric processing on P bioavailability are explored. The identification and categorization of the sources of P and its seasonal variation, influenced by meteorological conditions, are presented.

#### 2. EXPERIMENTAL SECTION

**2.1. Aerosol Sampling.** This study involved the simultaneous long-term sampling of aerosol particles at two sites: the Cape Verde Atmospheric Observatory (CVAO) in Cabo Verde and the Namib Desert Atmospheric Observatory (NDAO) located at the Gobabeb Namib Research Institute in Namibia (Figure 1). While the CVAO (16.8640° N, 24.8675°

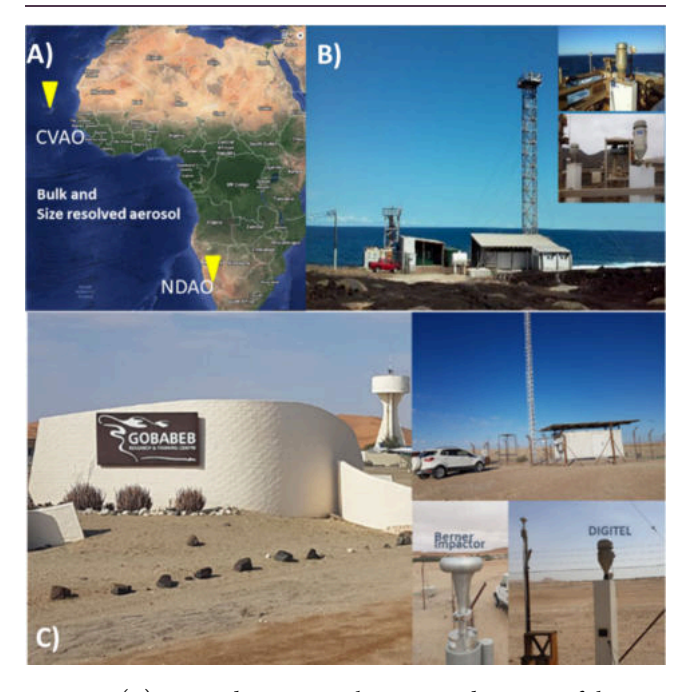


Figure 1. (A) Map indicating sampling sites and pictures of the sites and the samplers at (B) CVAO ( $16.8640^{\circ}$  N,  $24.8675^{\circ}$  W) and (C) Gobabeb, NDAO ( $23.5603^{\circ}$  S,  $15.0404^{\circ}$  E).

W) is exclusively located in the tropical North Atlantic about 900 km off the west African continent, the NDAO (23.5603° S, 15.0404° E) is located about 60 km inland from the southern African tropical coastline boundary (23.5° S) of the Atlantic. Sampling was done at these two sites considered to be representative of aerosol particles in the NETA and SETA regions, respectively, from the 5th of May 2018 to the 31st of December 2019. Continuous bulk  $PM_{10}$  aerosol samples were

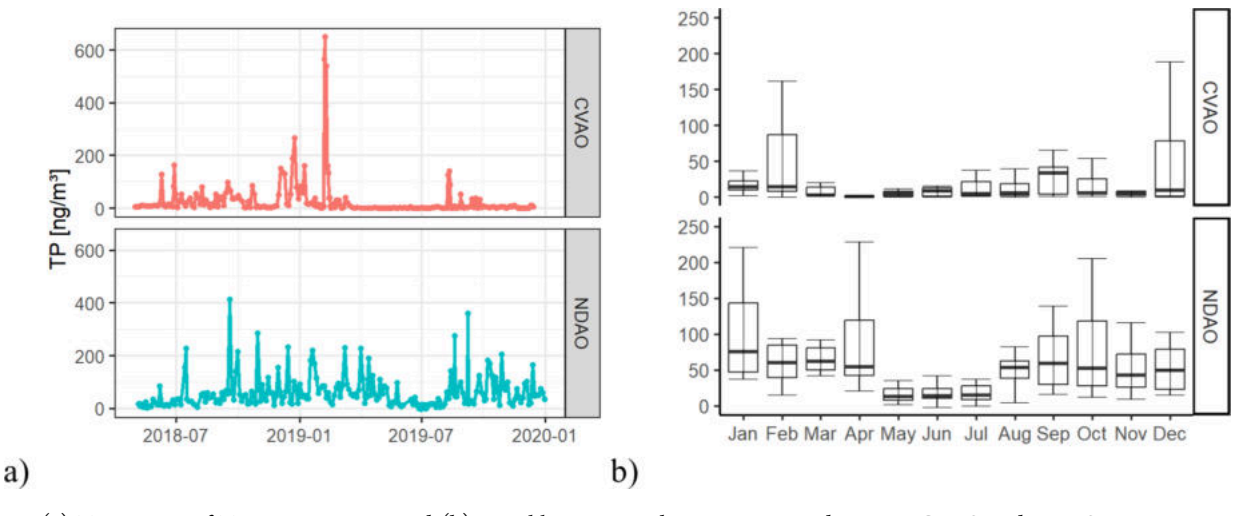


Figure 2. (a) Time series of TP concentrations and (b) monthly variations between 2018 and 2019 at CVAO and NDAO.

collected over 72 h at CVAO and NDAO by using a highvolume PM collector (DIGITEL DH80, Riemer, Germany) with preheated quartz fiber filters (Munktell, MK 360, Germany). During intensive field studies, each lasting 4-6 weeks in January and February 2019 at CVAO and July 2019 at NDAO, similar bulk samples were collected over a 24-h routine. In addition, during the intensive field studies, sizeresolved PM samples were collected with a PM<sub>10</sub> five-stage Berner Impactor (Hauke, Gmunden, Austria) with cut-offs at 50-140 nm, 420 nm,  $1.2~\mu$ m,  $3.5~\mu$ m, and  $10~\mu$ m on polycarbonate and aluminum foils (Wicom, Heppenheim, Germany). After collection, all samples were frozen and transported to TROPOS for laboratory analysis. For the quality control of the samples from both sampling instruments, field blank samples were collected and treated in the similar way as the samples. Field blanks are filters that were inserted into the samplers for the same sampling duration as the filter samples, 72 and 24 h for bulk and size-resolved samples, respectively, but no air sucked through them.

**2.2. Chemical Analysis.** Aerosol samples were analyzed for various P contents, including total, inorganic, organic, and soluble P. In addition, the samples were analyzed for their chemical compositions, including the quantification of water-soluble ions and organic compounds.

2.2.1. Phosphorus Analyses. For size-resolved samples, total phosphorus (TP) was quantified using a total X-ray fluorescence (TXRF) technique on particles collected on polycarbonate foils. Here about 0.25 cm² area of the foil is cut out and placed on a TXRF carrier, which was thereafter spiked with 5  $\mu$ L of gallium/yttrium internal standard mixture in concentrated nitric acid (69%, supraquality, ROTIPURAN, Roth, Germany) and allowed to dry on a hot plate. After cooling, the carrier was analyzed with the TXRF instrument (PICOFOX, Bruker Germany); details can be found in the literature. <sup>35</sup> PM<sub>10</sub> bulk samples were analyzed differently.

For the TP quantification of  $PM_{10}$  bulk aerosol samples, three 16 mm sections were punched out of the quartz filters, combusted at 500 °C for 2 h, and extracted in 3 mL of 35% concentrated HCl (supra-quality, ROTIPURAN, Roth, Germany). For the total inorganic phosphorus (TIP), a 16 mm filter punch was directly extracted in 1 M HCl for 2 h by shaking at room temperature, and thereafter the extracts were quantified.  $^{36,37}$ 

The extracts for the TP and TIP were quantified using the molybdenum blue method. Here 5 mL of each sample extract was incubated with 1 mL reagent containing sulfuric acid, ascorbic acid, potassium antimonyl tartrate trihydrate, and ammonium molybdate. The free phosphate reacts with the molybdenum species to form a molybdophosphoric acid compound, which is reduced by ascorbic acid to form a phosphor–molybdenum blue complex that is stabilized with antimony. The resulting blue complex was quantified using a UV–vis spectrometer (TIDAS, J&M Analytics, Germany) at 710 nm. To enhance the sensitivity of detection of the blue complex, a 100 cm Liquid Waveguide Capillary Cell (LWCC, World Precision Instruments, Germany) absorption cell was used. The limit of detection (LOD) was at 0.01  $\mu$ g of P/L.

Soluble phosphorus (SP) was analyzed using ion chromatography (IC) as well as the molybdenum blue method. A 5 cm filter punch was extracted in 20 mL of deionized water for 2 h by shaking at room temperature, filtered through a 0.45  $\mu$ m syringe, and measured with either IC or colorimetry. The remaining extracts were used for pH and sugar analysis. The results from both techniques were in good agreement and within an error range of 5%. Thus, the soluble P was routinely quantified by IC.

The filter blank values of SP (<0.09 ng/m³) and TP (<0.5 ng/m³) were very low, and the P retention capacity of the quartz filters were also low, with SP recoveries from 1 ppm spiked P standard solution on 16 mm quartz filter sections, ranging between 94 and 105% for a sample set of five filters.

Total organic phosphorus (TOP), was determined as the difference between TP and TIP. The uncertainties of the TOP concentrations were less than 6.5%, which was obtained from error propagation of the uncertainties of TIP (5%) and TP (4%) taken from replicates of blank filter measurements.

2.2.2. Analysis of Other Chemical Compounds. Watersoluble ions including dissolved nitrogen species ( $NH_4^+$ ,  $NO_2^-$ , and  $NO_3^-$ ) as well as  $SO_4^{\ 2^-}$ ,  $K^+$ ,  $Na^+$ , and  $Ca^{2^+}$  were quantified from the sample extracts in deionized water with an IC using reported procedures.<sup>39</sup> The nonsea salt (nss) fraction of a water-soluble ion was estimated as the difference between the measured ion concentration and the sea salt (ss) contribution to the ion concentration. Specifically, for  $SO_4^{\ 2^-}$  and  $Ca^{2^+}$ , the sea salt contributions, ss- $SO_4^{\ 2^-}$  and ss- $Ca^{2^+}$ , were calculated as  $0.25[Na^+]$  and  $0.04[Na^+]$ , respectively. This was done under the assumption that sea salt was the only source of

Na<sup>+</sup>. For organic and elemental carbon (OC/EC) analysis, we used a thermo-optical method following the EUSAAR II protocol to quantify the OC/EC of the quartz filters. The aerosol pH was determined from the water extracts of the samples using a Sartorius PP-20 pH meter. Anhydrous sugar compounds including levoglucosan, arabitol, and mannitol, were measured from the same SP extracts via anion-exchange chromatography using a high-performance anion-exchange chromatography coupled with a pulsed amperometric detection instrument ICS 3000 (Thermo Fischer).<sup>40</sup>

**2.3. Air Mass Back-Trajectories.** Air mass back-trajectories were determined using the NOAA HYSPLIT model<sup>41</sup> for 96 h using meteorological input data from the Global Data Assimilation System (GDAS, 1°), and a receptor height of 500 m above ground level. The trajectories were calculated every 4 h within the sampling period and were grouped into 4 clusters using the K-means algorithm approach 42–44 as well as geographical origin and trajectory path using the trajCluster script in the R-Studio Openair package. The P chemical components of the samples were combined with the assigned clusters of the samples. The combination of the clusters and the different P concentrations provided the relative contribution of the different air mass origins to the various P forms. Further details of the method have been published elsewhere.

# 3. RESULTS AND DISCUSSION

3.1. Phosphorus Concentrations. The time series of TP concentrations at NDAO and CVAO are presented in Figure 2a. At NDAO, TP concentrations ranged between 2 and 413  $ng/m^3$ , with an annual mean of  $62.8 \pm 28.2$   $ng/m^3$  for the sampling period. The TP showed a strong temporal variation, particularly during March and May of 2019, characterized by frequent concentration maxima and minima, likely associated with dynamic weather patterns such as dust storms and strong winds (>8 m/s) that increases ambient crustal material abundance. In comparison to similar measurements in southern Africa, the mean TP concentrations were higher than the  $31 \text{ ng/m}^3$  mean P reported in neighboring Zimbabwe, <sup>26,48</sup> and the 10 ng/m³ at the coastal Henties Bay observatory in Namibia. 49 The concentrations were, however, similar to those reported from other tropical regions such as Rondonia in Brazil, 67 ng/m<sup>3</sup>. <sup>26,50</sup> The baseline concentrations (considered as the fifth percentile of the concentrations) of P in this region was about 12 ng/m<sup>3</sup>. At CVAO, similar strong temporal variations as at NDAO were observed, with concentrations ranging from 0.2 to 650 ng/m<sup>3</sup> and an annual mean of 29.8  $\pm$  76 ng/m<sup>3</sup> for the observational period. Frequent peak observations were attributed to air mass influx from the Saharan/Sahel regions. The baseline concentrations at CVAO (1.2 ng/m<sup>3</sup>) were much lower than at NDAO. Apart from occasional spikes in the time series, the average concentration at NDAO was higher than at CVAO (Figure 2a), suggesting a greater contribution of atmospheric P sources in the SETA compared to the NETA regions. However, although these differences are eminent, the effective flux into the open ocean in the SETA region would be eventually lower than those observed at the NDAO due to its location on land compared to the CVAO site.

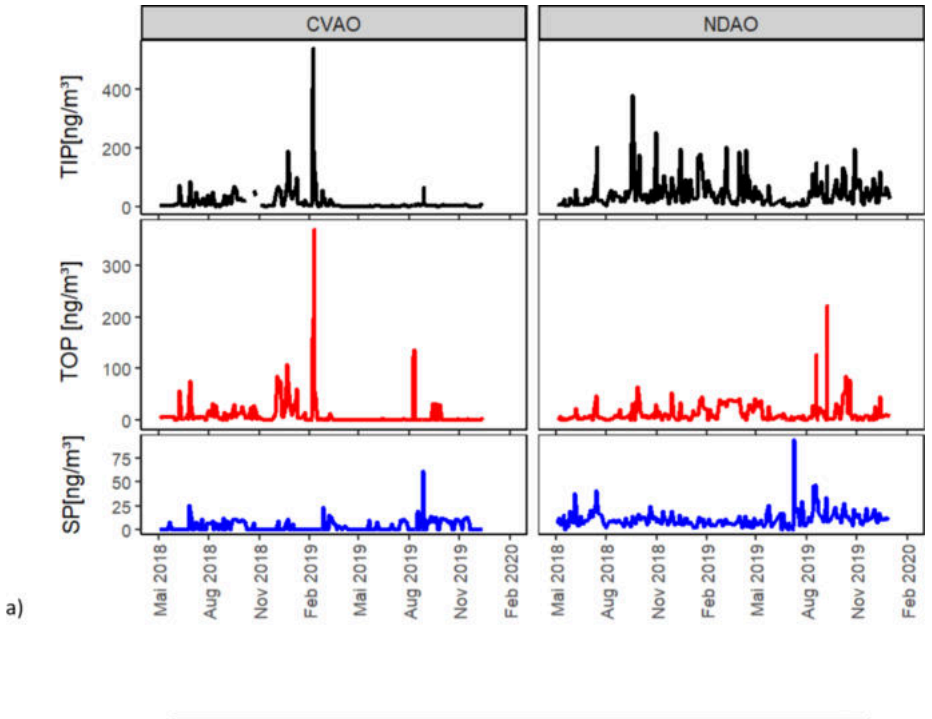
Table S1 compares the results of this study with those observed in other marine, coastal, and inland regions. The yearly average concentrations for TP observed at CVAO are higher than those reported for Miami, USA ( $11.8 \pm 9.7 \text{ ng/m}^3$ ;

 $380 \pm 312 \text{ pmol/m}^3)^{33}$  during Saharan dust episodes, and the range is about 2 orders of magnitude higher than those reported during ship cruises along the Atlantic with a range of only  $0.1-5.6 \text{ ng/m}^3$ . The CVAO mean concentrations are also higher than those reported in the South China Sea, <sup>51</sup> the Western North Pacific, and the Arctic Oceans <sup>52</sup> but similar to those of many studies in the Mediterranean region. <sup>53</sup> These differences may be due to the proximity of the CVAO to the Sahara Desert in comparison to other sites located far away from prominent dust sources. The NDAO concentrations were marked by influence of air masses from the southern African interior during biomass burning episodes and were lower than coastal sites in China, such as Qingdao, <sup>54</sup> but much higher than those reported during the fall at Cayenne (15–154 ng/m³) by Barkley et al. <sup>55</sup>

The seasonal trends in TP at NDAO (Figure 2b) showed on average higher concentrations during austral summer months (DJF) compared to fall (MAM) despite sporadic peaks in the fall months caused by intermittent sandstorms.<sup>56</sup> The highest ambient P loads were observed in January, and the minimum in May. Excluding the sudden peaks, the concentration range in May and June is relatively low, between 2 and 32 ng/m<sup>3</sup>. During the austral winter months, the concentrations are the lowest with a slight increase in August toward the end of winter, which on average is still lower than the summer months. These first observations of seasonal ambient P trends in this arid region suggest that regions close to the desert may not be solely influenced by local resuspension but can be strongly affected by regional wind patterns and other longrange transported air masses. The slight increase in TP in August was not always correlated with an increase in PM mass (Figure S1), suggesting that the PM mass was not mainly indicative of P abundance. Thus, long-range transport and mesoscale meteorology may play a more significant role in nutrient transport throughout the year than local emission patterns. However, the strong easterly transport that was observed in the summer and spring months from backtrajectories was accompanied by high loads of suspended dust particles, which could account for the higher observed summer TP concentrations.

At CVAO, the seasonal pattern revealed the highest concentrations in December to February (boreal winter) driven by the dust transport pattern in this region,<sup>57</sup> with February and April being the months of highest and lowest concentrations, respectively. The lowest concentrations are observed during the boreal spring, with a TP concentration range between 0.9 and 13 ng/m<sup>3</sup> from March to May. Comparing the concentrations observed at the two sites, the monthly TP concentration ratios (NDAO to CVAO) varied between 0.6 and 50, with the highest difference observed in April and the lowest in February. In February at CVAO, episodes of high Saharan dust are often observed, leading to elevated P concentrations compared to the other months and a lower ratio. Likewise, the higher ratio in April results from the lower background concentration of P at CVAO during this month, in contrast to relatively higher concentrations at NDAO. In general, the monthly average values at NDAO were often higher than those at CVAO due to different source regions, proximity to source regions, stronger influence of local winds and thus elevated resuspension at NDAO in comparison to a stronger reliance on long-range transport at CVAO.

**3.2. Temporal Variation of TIP, TOP, and SP.** Total inorganic, organic, and soluble P contents were quantified at



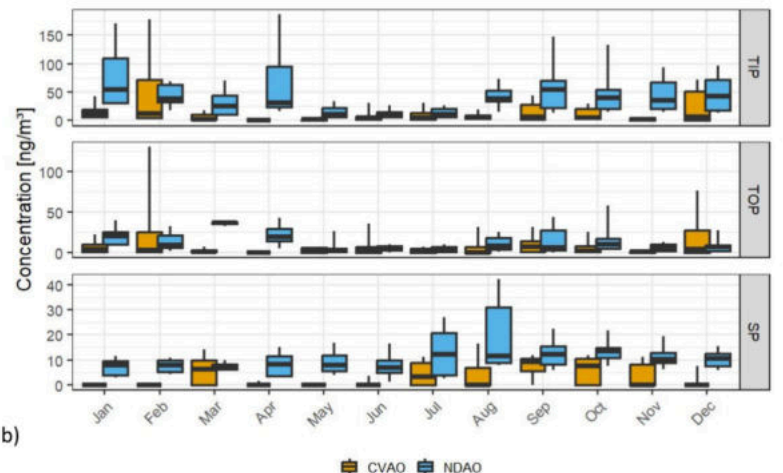


Figure 3. (a) Time series of TIP, TOP, and SP at CVAO and NDAO. (b) Monthly trends of the P components.

both sites. The time series of these components are shown in Figure 3a and their monthly trends in Figure 3b. Inorganic P (TIP) dominated the TP composition with concentrations ranging from 1 to 381 ng/m³ and from 0.1 to 540 ng/m³ at NDAO and CVAO, respectively, and showing strong correlation with TP concentrations at both sites ( $r^2 > 0.9$ ; p < 0.05). Peaks in TIP were observed during periods of high TP concentrations and the seasonal trends were similar. At CVAO, there was a strong coincidence between TIP and TOP peaks which was not observed at NDAO indicating that the sources of TIP and TOP at NDAO were not always the same.

In general, TOP concentrations reached up to 221 and 370 ng/m<sup>3</sup> at NDAO and CVAO, respectively, with TOP concentrations often lower than TIP and higher TOP observed at CVAO. On average, TOP was 19% of the TP at NDAO and about 39% at CVAO, indicating a higher contribution of particles containing organic P compounds at CVAO. These particles could be sourced from biogenic emissions of plant debris transported from Africa or Europe to CVAO, <sup>58</sup> while on

the contrary, the arid location of NDAO is not privy to such particle sources.

Soluble P (SP) also exhibits a strong temporal trend with higher values observed at NDAO (<94.2 ng/m³) compared to CVAO (<61.4 ng/m³). However, the days of high SP did not always coincide with days of higher TP at both sites, suggesting different source contribution influences.

The seasonal patterns of these P forms (Figure 3b) reveal similar trends between TIP and TOP, with peaks observed in the boreal winter and early fall and the lowest concentrations observed in the boreal spring at CVAO. However, the SP trend showed the highest concentrations in the boreal summer, specifically in August and September at CVAO. This indicates that high TP content does not necessarily imply a high soluble fraction of P, which is critical for primary productivity in marine and terrestrial ecosystems.

Similarly, at NDAO, the seasonal trends for TIP and TOP were similar, with peaks in early fall and spring and low concentrations in the Winter months. However, SP concentrations peaked in the Winter and Spring months, in contrast

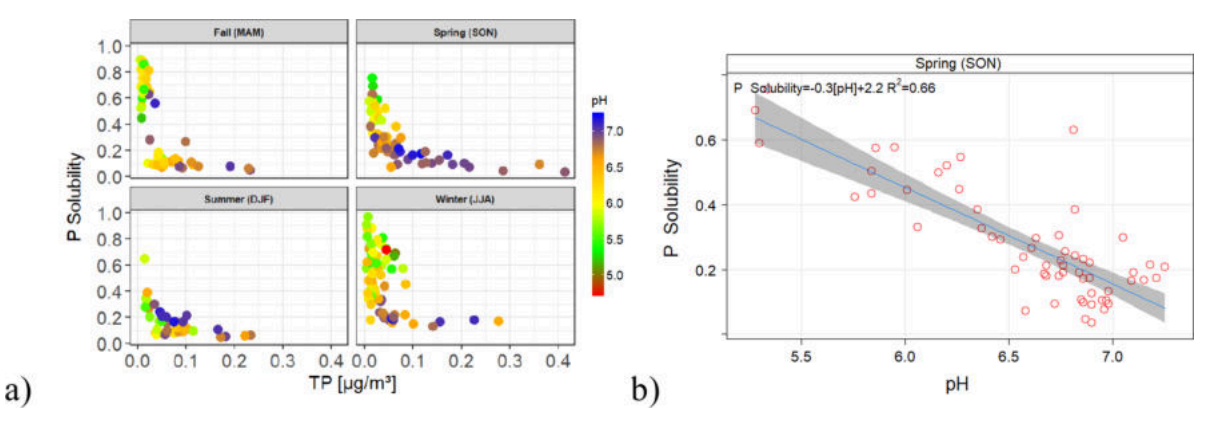


**Figure 4.** (a) Inverse seasonal relationships between TP and the solubility of P according to the pH of the samples at NDAO. (b) Linear relationship between the solubility and aerosol particle's pH observed at NDAO between September and November. The blue line represents the fitted regression line, while the shaded area is the 95% confidence interval of the fit.

to the TIP and TOP trends. This discrepancy in the seasonal trend is linked to different activities and emission sources. During the winter and early spring months, peak levoglucosan (a marker for biomass burning) concentrations (Figure S2) are observed in July and August indicating high combustion activities, especially from biomass burning. This suggests that aerosols from combustion carry more soluble P than other aerosol sources during other months, leading to the strong winter peaks of SP.

In comparison to other studies (Table S1), the SP concentration at NDAO (10.5  $\pm$  9.3 ng/m³) is higher than those in Miami (3.1  $\pm$  2.8 ng/m³) and Barbados (2.6  $\pm$  1.3 ng/m³)³³) but similar to that at the Gulf of Aqaba (12.4  $\pm$  6.2 ng/m³). The SP value at CVAO (3.3  $\pm$  6.4 ng/m³) was similar to those reported for Miami. The SP concentrations at both sites were lower than that reported for Qingdao in China (21.8  $\pm$  21.4 ng/m³). These results highlight the importance of long-term measurements in comparison to snapshot observations to assess seasonal patterns and processes that affect long-term P fluxes to the oceans.

**3.3. Size Distribution of TP.** During intensive field studies at NDAO in July 2019, and January and February 2019 at CVAO, the size distribution of P was quantified using TXRF on size-resolved aerosol samples collected with a 5-stage Berner Impactor.<sup>60</sup> TP concentrations were highest in the coarse mode fraction at both sites (Figure S3). Higher coarse mode abundance was observed at the CVAO compared to the NDAO likely due to the sampling seasons, with higher Saharan dust influence in February at the CVAO compared to Namibian dust influence in July at the NDAO. However, the fine-to-coarse mode ratio  $(PM_{1.2}/\ PM_{10})$  of the particles ranged between 0.14 and 0.61 with an average of 0.39  $\pm$  0.17 at NDAO and between 0.07 and 0.29 with an average of 0.15  $\pm$  0.05 at CVAO with the lowest ratios typically observed during dust events. The fine mode fraction was elevated for particles between 420 and 1200 nm in size and represented 20% and 35% of the TP at CVAO and NDAO, respectively. This indicates that a significant amount of fine-mode particles contributed to the P budget. Typically, fine-mode particles often originate from combustion, which supports our interpretation above about the role of biomass burning and particle size in influencing the soluble P content. Studies have also reported correlations between P solubility and the specific surface area of aerosol particles, with solubility increasing with decreasing size of dust particles.<sup>54</sup>

**3.4. P Solubility.** The solubility of P (SP/TP) was evaluated and its relationship with TP was examined. The solubility showed an inverse relationship with the  $PM_{10}$  concentrations at both sites (Figure S4a).

Figure 4a) illustrates the fractional solubility plotted against the TP of samples during different austral seasons at NDAO (months abbreviated in brackets) with the color of a sample representing its pH. The strong inverse relationship between the solubility and TP indicates that the P solubility is higher for samples with lower TP and lower for samples with higher TP. Similar inverse relationship was also observed for samples collected at the CVAO (Figure S4b). During intensive campaign periods when size-resolved measurements were conducted, the fine-to-coarse mode ratio was frequently higher on days with lower TP, suggesting that fine particles contributed to the enhanced solubility observed during these periods. In austral spring (September, October, and November), a linear relationship was observed between the aerosol pH and P fractional solubility (Figure 4b), suggesting that other processes than TP content alone contribute to P solubility. Generally, whenever the pH of the particles was less than 5.8, the solubility was typically above 40% (0.4), which often occurred during the austral winter and spring seasons. Similar inverse relationships were observed between total iron and its fractional solubility 61,62 and fractional solubility of P and total aluminum, used as a marker for dust mass concentration in Asian dust particles.<sup>54</sup>

Atmospheric processing at the surface of P-containing particles likely affects P solubility through interactions between the particles and acidic species leading to a release of labile P. The observed relationship is likely driven by smaller particles with a higher surface area-to-volume ratio, which are known to dominate surface reactive processes. According to previous laboratory studies, the solubilization of P and its subsequent release from dust particles can depend on the concentration of hydrogen ions (acidity) in the surrounding aqueous layer.<sup>32</sup> High P and calcium solubility, was observed at lower pH, suggesting a reaction between the acidic centers of the phosphate and OH or F groups of apatite minerals at the surface that weakens the calcium bonds and enhances the mobilization of P from the crystal structure into the solution. Our results (Figure 4b) suggest a similar explanation especially since these processes may be further enhanced at high temperatures typical for combustion processes.

During combustion, organic matter and soil particles are emitted into the atmosphere, including trace gases such as SO<sub>2</sub> and nitrogen oxides (NO<sub>x</sub>), which can be further oxidized to form sulfuric and nitric acids.<sup>63</sup> These acids can readily be adsorbed by the aqueous film at the surface of the particles, creating an acidic shell over the particles that stimulate chemical reactions. At lower pH, a higher content of anions (nss-sulfate and nitrate ions) is observed, and soluble P showed a good correlation with these ions. Figure S5 illustrates the relationship between P solubility and the molar ratios of acidic species (sum of nss-sulfate and nitrate) to TP, revealing a good linear correlation ( $R^2 = 0.67$ ; p < 0.05) between TP, acidic species, and P solubility despite the high scattering observed especially in the spring data (Figure S5). This correlation is particularly evident during seasons of enhanced P solubility (e.g., spring), suggesting that acidic precursors of these species play a role in enhancing the mobilization of P from its matrix and substantiating the results for pH dependence (Figure 4b).

The aerosol pH and acidic content may also be influenced by aerosol cloud interactions during the long-range transport of particles.<sup>64</sup> In principle, during aqueous—phase reactions in cloud droplets, secondary organics including organic acid precursors and sulfates are formed, which can accumulate on particles after the evaporation of cloud droplets, enhancing the chemical and acidic content of aerosol particles.<sup>32,64–66</sup> Although cloud occurrences are not frequent at NDAO, greater seasonal occurrences during the austral spring (September to November) were reported by Andersen et al.,<sup>67</sup> which suggests that cloud dissipation might have also contributed to enhanced particle acidity and the more pronounced P-solubility observed during these months.

Nevertheless, in addition to the influence of aerosol acidity on P solubility, the sources of the particles and their sizes also play a significant role in the fate of these particles, due to the forms in which the respective P compounds are available. According to Mahowald et al.,<sup>68</sup> mineral dust particles are generally less soluble compared to PM from other sources such as combustion, traffic, or industrial plants, which are often fine. Likewise, Shi et al.<sup>54</sup> showed that P from anthropogenic sources often have elevated solubility to those of mineral dust particles, as they loosely associate with PM particles and can dissolve more readily in comparison to P in minerals, thereby reacting more easily with acidic precursors to provide more soluble P.<sup>23,51,69,70</sup>

A time series plot (Figure 5) explored the interrelationship between solubility and combustion and other nonmineral dust P sources by examining the fractional solubility alongside levoglucosan and aribitol, which are markers for biomass burning and fungal spores, respectively. Periods of high P solubility at NDAO coincided with increases in levoglucosan and arabitol concentrations in the samples, thereby suggesting that biomass burning may serve as a source of phosphorus and/or enhance its solubility.

The enhanced availability of acid precursors and their subsequent condensation on dust particles in association with higher combustion temperatures may favor the dissolution and mobilization of labile P at the surface of dust particles from their source minerals, thereby increasing the soluble fraction. In addition, particles emitted due to combustion tend to be finer, hence increasing their solubility due to their increased surface-area-to-volume ratio and abundance in the 0.45  $\mu$ m sample extracts. It has been observed that biomass burning in

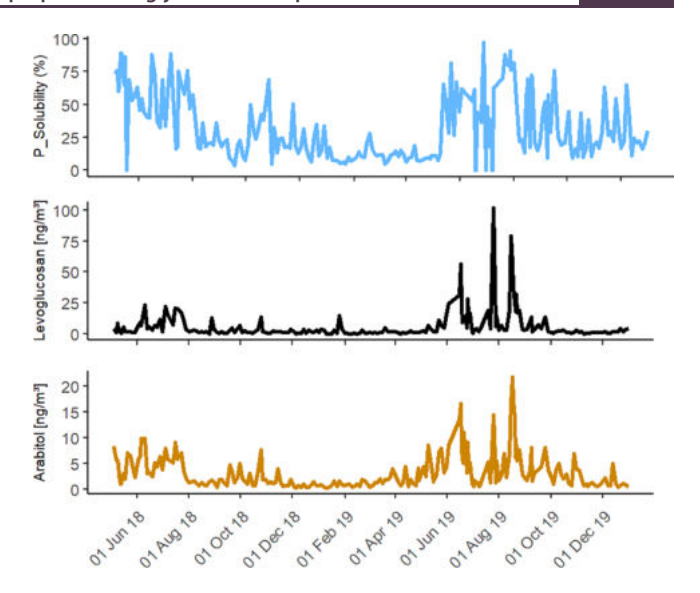


Figure 5. Temporal variation of P solubility, levoglucosan, and arabitol at NDAO.

Africa could significantly contribute to high levels of soluble phosphorus, with strong impacts on the Amazon rainforest, with African sources accounting for about half of the annual phosphorus deposition in the Amazon. It indicates that biomass burning has a greater role in the local biogeochemical system as it increases the solubility of P in ambient particles.

The correlation between higher P solubility and arabitol emphasizes the role of biogenic sources and emissions on P solubility. Diao et al. highlighted the role of primary biological aerosol particles containing P as an important source of bioavailable P, while SP flux calculations from Myriokefalitakis et al. assumed that 50% of fungal spores were soluble. These studies highlight the role of fungal spores in enhancing P solubility at NDAO site. The good coincidence between the variations in aribitoal and levoglucosan further suggests the role of biomass burning in transporting fungal spores, highlighting its dual influence on P solubility.

**3.5. Sources of Phosphorus.** We employed air mass trajectory and correlation analyses to identify the potential sources and source regions that contributed to the observed concentrations of P species.

3.5.1. Influence of Air Masses. Back-trajectories were clustered based on the frequencies of air mass passage over specific geographical areas to provide an average representation of trajectory groups with distinct geographic patterns. The openair package of the R software was used for this clustering process.<sup>47</sup> Parts a and b of Figure 6 show the main origins of air masses at the CVAO and NDAO during the study period, while parts c and d of Figure 6 show the contributions of these air masses to the total, soluble, and organic P budgets observed at the respective sites. At NDAO, 61% of the air masses originated from the southern oceans and traversed the length of the coastal Namib Desert Sand Sea before arriving at the site (Figure 6b). The southern African interior, which typically carried high elemental carbon and levoglucosan from biomass burning and PM from industrial activities, transport, and intensive agriculture<sup>49</sup> accounted for 17% of the air masses, while 16% originated from the central South Atlantic Ocean (western inflow) crossing coastal cities before arriving at the site, and 6% of the air masses had south and northwest inflow characteristics. These four clusters described the general air

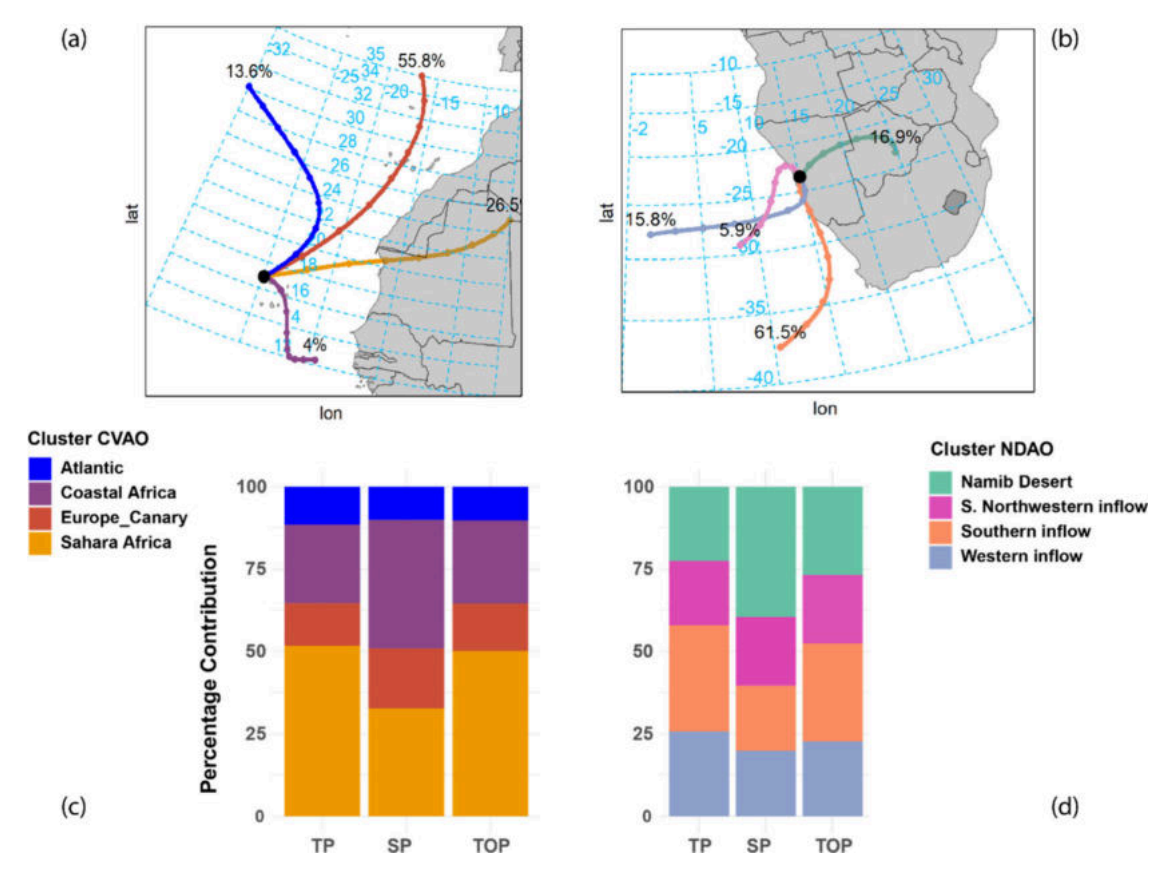


Figure 6. Air mass back-trajectory clusters and their relative frequencies of occurrences at (a) CVAO and (b) NDAO during the study period, with respective contributions of the air masses to TP, SP, and TOP at (c) CVAO and (d) NDAO. The colors represent the clusters and their origins.

mass inflow during the study period at NDAO. The southern air masses contributed about 32% to the TP (Figure 6d), while the air masses from the west and the continental interior from the east contributed about 26% and 23% to the TP, respectively. This indicates that TP is strongly influenced by oceanic and coastal factors, including influences from coastal anthropogenic activities and the dunes along the Namibian coastlines.

At CVAO (Figure 6a), most of the air masses originate from the Canary Island region, accounting for about 56% of the total air masses observed, followed by air masses from continental North Africa (26%), often laden with Saharan dust particles.

Air masses originating from coastal West Africa through Cabo Verde or from the Central North Atlantic Ocean only account for about 4% and 14% of the total air masses, respectively. Most of the TP at CVAO originated from continental Africa (52%), predominantly during periods of Saharan dust outbreaks when TP concentrations increased about 10-fold compared to the baseline concentrations typically observed during coastal African and North Atlantic air mass influences. Air masses from Europe, crossing the Canary Islands to CVAO and those from coastal Africa, also carried significant TP 13% and 24%, respectively, from anthropogenic activities (Figure 6c).

The SP and TOP contents also showed strong variations with the air mass origins. While TP and TOP concentrations were higher during the inflow of continental air masses from the Sahara and North Africa at CVAO, SP concentrations were higher (39%) in air masses originating from coastal western Africa that crossed over the Cape Verde Islands before arriving at the sampling site (Figure 6c). The highest SP was associated

with such air masses as the TP content was typically low. These air masses contained higher concentrations of combustion markers such as nonsea salt potassium and elemental carbon (levoglucosan was not analyzed for all these samples). When mineral dust (identified by high nonsea salt calcium content) was mixed with aerosols derived from combustion, the SP content was also elevated. Consequently, air masses from continental North Africa ranked second in terms of SP content.

At NDAO, the SP and TOP patterns were similar for dominant air masses (Figure 6d). However, air masses originating from the southern African interior, which also traversed regions with large industrial centers and high-density rural and urban populations that typically use wood biomass for energy before reaching NDAO, transported higher levels of SP. These air masses from the east contributed approximately 39% of the observed SP and accounted for about 61% of levoglucosan occurrence at the site. The average pH of the particles associated with these air masses was the lowest at about pH 6.01, indicating their weak acidic nature. These results confirm that combustion sources and processes contribute significantly to the soluble P observed in this region. In summary, we conclude that continental air masses carrying particles from sources of biomass or wood combustion typically carry high SP content and have higher particle acidity, resulting in greater P solubility than air masses from dust events that carry mostly minerals rich in P with high TP content but lower solubility.

3.5.2. Organic and Inorganic Phosphorus. To assess the influence of mineral dust on the TOP content in the samples, we compared the TOP: Ca ratios with the TOP: OC ratios.

There was a good correlation between these ratios ( $r^2 = 0.8$ ; p < 0.05), especially during the Austral spring (SON) and summer (DJF) periods, indicating that elevated levels of organic phosphorus were associated with dust transport, particularly at NDAO. The correlation of TOP with levoglucosan, indicative of biomass burning, was weak, suggesting that biomass burning was not a significant source of TOP. However, TOP was also detected during periods of marine air mass inflow, suggesting that marine aerosol particles could contribute to the TOP content.

It is worth noting that the P content in sea spray particles is typically low. However, marine aerosol particles can be released into the atmosphere from the sea surface microlayer, a known habitat for marine life including bacteria and other Pcontaining organic compounds<sup>72</sup> derived from processes such as phytoplankton cell lysis.<sup>73</sup> During aerosol formation processes such as bubble busting or wave breaking, these materials can be incorporated into the aerosol particles, thereby contributing to the atmospheric P budget. Phosphine has also been reported to contribute to P concentrations in other marine environments.<sup>74</sup> Although we cannot conclude that these processes contributed to the P budget at the sampling sites, they could account for TOP content in marine air masses. Furthermore, studies have identified the presence of soil microorganism in mineral dust particles, which may contain phosphorus in their structures, contributing to the organic phosphorus budget of dust particles.<sup>75,76</sup>

TIP was correlated with nonsea salt calcium (nss-Ca), to assess its association with mineral dust particles. The correlations with fluoride and nss-Ca (Figure 7), with regression coefficients  $(r^2)$  of about 0.8, indicate a strong correlation between these species.

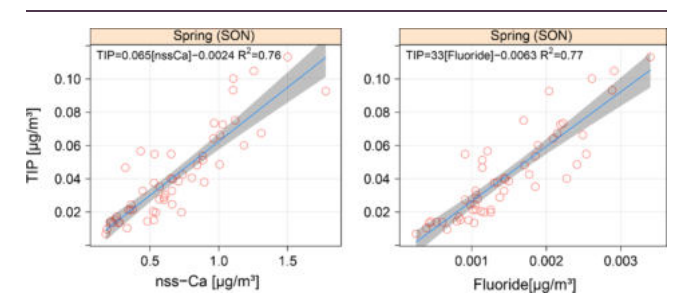


**Figure 7.** Correlation plots between TIP and nonsea salt calcium and fluoride at NDAO during September, October, and November.

The strongest correlation was found during the austral spring at NDAO. This robust correlation between TIP, nss-Ca, and fluoride suggests the presence of FAP  $[Ca_5(PO4)_3F]$  minerals in the aerosol particles of this region. A recent study on aerosols at Henties Bay, coastal Namibia, also found elevated fluoride concentration in Namibian dust supporting the observations of this study. The influence of crustal minerals, particularly apatite, on the inorganic P content has been observed in other regions, such as the Saharan and Middle East regions. In this study, we confirmed a similar association in the Namib Desert region. A similar trend in the correlation between TIP and nss-Ca was also found at CVAO, suggesting a similar influence of apatite minerals originating from mineral dust, in both sampling regions.

**3.6. Deposition Fluxes.** The time series of TP deposition fluxes (Figure 8) at CVAO and NDAO were estimated using the approach of Stokes et al. <sup>79</sup> In this method, the deposition

flux  $F_d$  is given as  $F_d = (C_C \times 2.0) + (C_f \times 0.1)$ , where  $C_C$  and  $C_{\rm f}$  are the concentrations of TP in the coarse and fine fractions and 2.0 and 0.1 cm/s are their respective depositional velocities. These literature values were chosen as their application meets with spokes et al. 79 assumptions for particles >1  $\mu$ m and deposition less than 1000 km from the land. However, these values may change with size fraction, hence, where possible, measured values should be considered in place of these given values. The mean coarse-to-fine mode ratio of P was about 0.61 at NDAO and about 0.85 at CVAO, which were used to estimate the fluxes. We also evaluated the depositional flux of dissolved inorganic nitrogen (DIN) and soluble phosphorus (DIP) to quantify the DIN:DIP ratios. Here, the mean depositional velocities of 0.23 cm/s for ammonium and 1.54 cm/s for nitrite and nitrate, were estimated based on their coarse-to-fine mode ratios during the intensive campaigns and the value for DIP was 1.14 cm/s. The values were similar to those reported in the literature.<sup>80</sup> The average values used have uncertainties (variations) of up to 60% driven by the temporal variation of the size distribution of the chemical components. However, the values of these studies are still comparable with other studies, since similar temporal variations are experiences in long-term observations.

The depositional fluxes at NDAO exhibited stronger variation throughout the year than those at CVAO. The TP fluxes ranged from 0.001 to 14.5  $\mu$ mol/m<sup>2</sup>·d, with an annual average of 2.0  $\pm$  2.2  $\mu$ mol/m<sup>2</sup> d, at NDAO and from 0.007 to 22.8  $\mu$ mol/m<sup>2</sup>·d, with an average annual flux of 1.0  $\pm$  2.7  $\mu$ mol/m<sup>2</sup>·d, at CVAO. Similarly, the DIP fluxes at NDAO were  $<1.1 \ \mu \text{mol/m}^2 \cdot \text{d}$  with an average of  $0.14 \pm 0.11 \ \mu \text{mol/m}^2 \cdot \text{d}$ and at CVAO <0.70  $\mu$ mol/m<sup>2</sup>·d with an average of 0.04  $\pm$  0.07  $\mu$ mol/m<sup>2</sup>·d. DIN fluxes ranged from 2.4 to 50.2  $\mu$ mol/m<sup>2</sup>·d and from 3.7 to 53.3  $\mu$ mol/m<sup>2</sup>·d at NDAO and CVAO, respectively. The TP fluxes at CVAO followed a strong seasonal pattern with maximum deposition in the boreal winter. In contrast, at NDAO, the austral spring and fall were the seasons of highest P deposition. The deposition of P in the NDAO region was generally higher compared to the CVAO region due to more frequent enhanced P concentrations throughout the year. In contrast, at CVAO, most of the P deposition occurred during dust storms that were dominant in the winter season. The TP depositional fluxes at CVAO are higher than those reported in the North Atlantic (0.064 mmol/ m<sup>2</sup>·yr) in Miami and Barbados (0.25–0.56  $\mu$ mol/m<sup>2</sup>·d)<sup>33,81</sup> but lower than those (<3.13 mmol/m<sup>2</sup>·yr) observed in the Mediterranean region. 80 The average DIP fluxes at CVAO were similar to those reported in Miami and Barbados (0.02-0.10  $\mu$ mol/m<sup>2</sup>·d)<sup>33</sup> but lower than at NDAO and those reported at Mt. Gongga (28 mg/m<sup>2</sup>·yr).<sup>27</sup> The NDAO values were comparable to those found in Finokalia (0.08 mmol/m<sup>2</sup>· yr), but lower than those at Erdemi (0.22 mmol/m<sup>2</sup>·yr).<sup>80,82</sup> Likewise the NDAO values were similar to those reported in the Bay of Bengal (2.3  $\pm$  0.9  $\mu$ mol of P/m<sup>2</sup>·d) but higher than those reported in the Arabian Sea (0.6  $\pm$  0.2  $\mu$ mol of P/m<sup>2</sup>· d).83 These differences are related to the different P sources and their respective relative contributions in various regions.

**3.7.** Implication for Marine Productivity. Optimum marine productivity is expected when marine waters have a N:P ratio of about 16:1, according to the Redfield ratio, with further requirements for micronutrients such as iron and cobalt.<sup>84</sup> Deviation from the Redfield ratio may indicate a limitation of one of the (micro-) nutrients. Nitrogen-fixing bacteria, such as cyanobacteria, convert atmospheric nitrogen

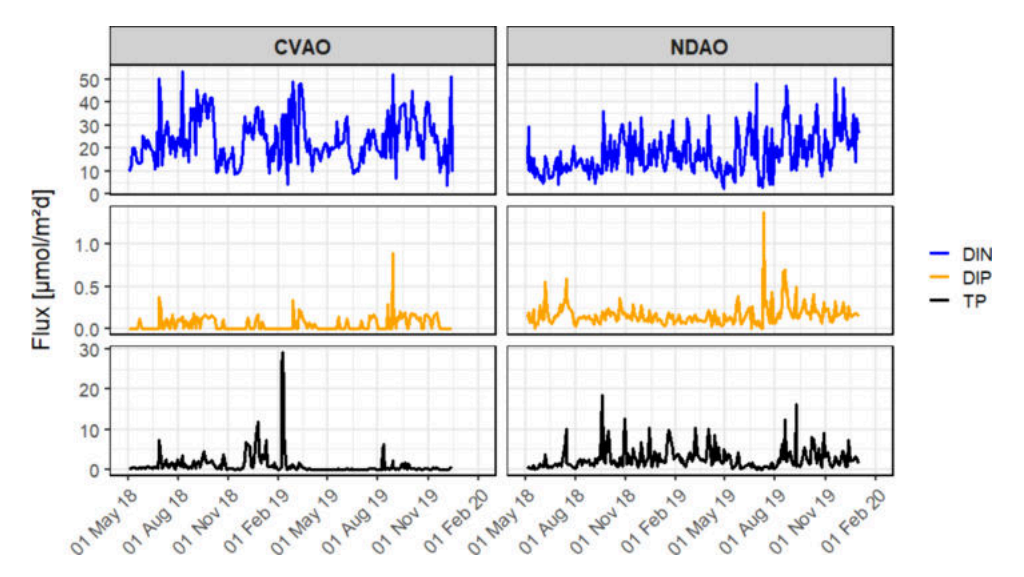


Figure 8. Time series of deposition fluxes in TP, DIP, and DIN at CVAO and NDAO.

to ammonia, through nitrogenese enzymes, if they have a sufficient supply of P and iron. 85 Atmospheric deposition of P, therefore, plays a crucial role in this process.<sup>86</sup> The molar atmospheric DIN:DIP ratios at NDAO exhibited strong fluctuations, ranging from 19 to 576, with an average of 191  $\pm$  115 and a baseline of about 52. The high ratios suggest that atmospheric deposition of P in this region is insufficient to reduce its deficiency relative to nitrogen and that P limitation will increases due to enhanced N input. The monthly average (Figure S6) highlights the seasonal variability, with lower DIN:DIP ratios in July-September (57-72) compared to June (147). At CVAO, ratios ranged from 60 to 486, averaging 249  $\pm$  84 with the lowest ratios observed in May (82) and the highest in January (271). The ratios at both sites are within the range reported in the Mediterranean (49-286)<sup>80</sup> and China's Coastal Seas (>100)<sup>87</sup> but higher than those recorded on the island of Crete (152).<sup>82</sup> The ratios are, however, lower than those in some coastal regions including Barbados (>500)<sup>33</sup> and Erdemli (261).82

Assuming the DIP and DIN fluxes become bioavailable for primary production and applying the Redfield stoichiometry for optimal biological productivity (C:N = 106:16 and C:P = 106:1), the theoretical new primary production from depositional fluxes of DIP and DIN in the Benguela marine ecosystem near NDAO will range from <1.4 mg of  $C/m^2 \cdot d$  and 0.19-3.98 mg of C/m<sup>2</sup>·d, respectively, and from <0.89 mg of  $C/m^2 \cdot d$  and 0.29-4.21 mg of  $C/m^2 \cdot d$  at CVAO, respectively, assuming insufficient P and N supply from other sources. Upwelling of nutrient-replete subsurface waters along the coast of Namibia increases DIN and DIP concentrations in the Benuela, but insufficient iron limits phytoplankton growth close to the coast and a gradual shift toward nitrogen limitation in the South Atlantic gyre with its nitrate-depleted waters.<sup>84</sup> Atmospheric inputs supplying iron would therefore benefit primary productivity in near-shore waters, and further offshore with nitrogen supply. The Benguela marine ecosystems will not necessarily benefit from the atmospheric P supply as atmospheric deposition would contribute less P and trigger less additional productivity than the rivers and upwelling inputs in this region. Atmospheric deposition, however, can be critical in the open oceans far from the shore or coastal areas

with rare fluvial inputs, such as the Benguela ecosystem in the NDAO region.

In contrast, the atmospheric inputs to the waters in the North East Atlantic directly benefit from both the atmospheric N and P inputs as the surface waters are depleted in nitrate and phosphate to nanomolar levels, which limits primary productivity and nitrogen fixation (in the case of phosphate availability). This indicates that atmospheric nutrient deposition can alter and benefit the local ecosystems by providing the required P for primary production and nitrogen fixation away from the NDAO and CVAO sampling sites.

In addition, as the NDAO is situated in an arid region, the varying DIN:DIP ratio would also affect nutrient balance in the surrounding terrestrial ecosystems, which may change terrestrial productivity, especially for arid plants, as well as variations in trophic interactions and ecosystem dynamics.<sup>89</sup> Unbalanced N:P ratios have been shown to negatively affect plant biomass, leaf area, and nutrient concentration in tissues of alpine species, indicating the considerable impact that atmospheric deposition may have on terrestrial ecosystems. 90 This effect would be negligible in agricultural fields as fertilizer treatments provide higher concentrations than those derived from atmospheric deposition. These likely effects on ecosystem productivity highlight the significance of long-term monitoring of biogeochemical fluxes in the atmosphere to enhance the predictability of the role of atmospheric deposition for validation of various models to improve the reliability of long-term forecasts in these regions of the Atlantic Ocean and elsewhere.

## 4. CONCLUSIONS

This study presents the first comprehensive analysis of P speciation including TP, TIP, TOP, and SP, across the Northeastern and Southeastern tropical Atlantic regions, particularly the important West African and Benguela marine ecoregions at CVAO and NDAO, respectively. Seasonal trends, source contributions, atmospheric processes influencing P solubility, and potential implications on ocean fertilization on adjacent marine ecosystems were investigated by quantifying the annual and seasonal fluxes of P in these two oceanic regions. The results show higher mean P concentrations at NDAO (56.1  $\pm$  62 ng/m³) compared to CVAO (29.8  $\pm$  76

ng/m<sup>3</sup>) with different seasonal trends. These differences were linked to air mass trajectories from source regions and proximities to their locations. Despite the high dust levels and the influence on P concentrations, the values of these study were still lower than those reported in many regions in China likely due to higher pollution from biomass burning and other industrial activities. While the main source of P in the Northeastern Atlantic region at CVAO was Saharan dust, a combination of Namib dust and anthropogenic biomass burning sources from the continental interior of southern Africa contributed to the P abundance at NDAO. Organic P could account for 19% and 39% of the total P in the NDAO and CVAO, respectively. The higher organic P content at CVAO was likened to its proximity to the ocean and frequent inflow of air masses from terrestrial regions. Soluble P was higher at NDAO (10.45  $\pm$  9.3 ng/m<sup>3</sup>) in comparison to the CVAO  $(3.3 \pm 6.4 \text{ ng/m}^3)$  driven by the stronger influence of anthropogenic sources and biomass burning. The good correlation between soluble P and levoglucosan, a biomassburning marker, as well as between soluble P and pH highlighted the role of combustion and atmospheric processing in enhancing P solubility. A significant source of P in both regions was mineral apatite as strong correlations were observed between P and apatite constituents. At CVAO, dry deposition could contribute to additional primary production, with estimated carbon fixation of up to 4.21 mg of C/m<sup>2</sup>·d, which is important for marine biogeochemistry in the nitrateand phosphate-depleted waters of the Northeast Atlantic and marine productivity in the West African Marine Ecoregion. At NDAO, due to its distance from the ocean, aerosol deposition also affects arid terrestrial ecosystems by contributing to nutrient balance and carbon budgets.

The study emphasizes the need for long-term monitoring of atmospheric nutrient fluxes to refine biogeochemical models and advance our understanding of their effects on marine and terrestrial ecosystems, thereby improving the predictability of their impacts.

## ASSOCIATED CONTENT

# Supporting Information

The Supporting Information is available free of charge at https://pubs.acs.org/doi/10.1021/acsearthspace-chem.4c00411.

Additional figures on P solubility and PM chemical constituents and a table comparing results with those of other studies (PDF)

# ■ AUTHOR INFORMATION

## **Corresponding Authors**

Khanneh W. Fomba — Atmospheric Chemistry Department, Leibniz Institute for Tropospheric Research (TROPOS), 04318 Leipzig, Germany; o orcid.org/0000-0002-4952-4863; Email: fomba@tropos.de

Hartmut Herrmann – Atmospheric Chemistry Department, Leibniz Institute for Tropospheric Research (TROPOS), 04318 Leipzig, Germany; ⊚ orcid.org/0000-0001-7044-2101; Email: herrmann@tropos.de

## Authors

Daniel T. Quaye – Atmospheric Chemistry Department, Leibniz Institute for Tropospheric Research (TROPOS), 04318 Leipzig, Germany Eric P. Achterberg – GEOMAR Helmholtz Centre for Ocean Research Kiel, 24148 Kiel, Germany; orcid.org/0000-0002-3061-2767

Eugene Marais — Gobabeb—Namib Research Institute, Walvis Bay 13013, Namibia; orcid.org/0000-0001-7155-9942

Complete contact information is available at: https://pubs.acs.org/10.1021/acsearthspacechem.4c00411

#### **Author Contributions**

The manuscript was written through the contributions of all authors. All authors have approved the final version of the manuscript.

#### **Notes**

The authors declare no competing financial interest.

#### ACKNOWLEDGMENTS

We thank the German Research Foundation (DFG) for financial support (Project: "PHOSDMAP" number FO 1106/2-1). In addition, the authors thank Susanne Fuchs, Anke Rödger, René Rabe, Marie Leinbweber, and Kornelia Pielok for their assistance during sampling and laboratory analysis.

### REFERENCES

- (1) Duhamel, S.; Diaz, J. M.; Adams, J. C.; Djaoudi, K.; Steck, V.; Waggoner, E. M. Phosphorus as an integral component of global marine biogeochemistry. *Nat. Geosci.* **2021**, *14* (6), 359–368.
- (2) Browning, T. J.; Moore, C. M. Global analysis of ocean phytoplankton nutrient limitation reveals high prevalence of colimitation. *Nat. Commun.* **2023**, *14* (1), 5014.
- (3) Paytan, A.; McLaughlin, K. The oceanic phosphorus cycle. *Chem. Rev.* **2007**, *107* (2), 563–576.
- (4) Tyrrell, T. The relative influences of nitrogen and phosphorus on oceanic primary production. *Nature* **1999**, *400* (6744), 525–531.
- (5) Diao, X.; Widory, D.; Ram, K.; Tripathee, L.; Bikkina, S.; Kawamura, K.; Gao, S.; Wan, X.; Wu, G.; Pei, Q.; Wang, X.; Cong, Z. Atmospheric phosphorus and its geochemical cycling: Fundamentals, progress, and perspectives. *Earth-Sci. Rev.* 2023, 243, No. 104492.
- (6) Benitez-Nelson, C. R. The biogeochemical cycling of phosphorus in marine systems. *Earth-Sci. Rev.* **2000**, *51* (1–4), 109–135.
- (7) Baker, A. R.; French, M.; Linge, K. L. Trends in aerosol nutrient solubility along a west-east transect of the Saharan dust plume. *Geophys. Res. Lett.* **2006**, 33 (7), No. L07805.
- (8) Baker, A. R.; Jickells, T. D.; Witt, M.; Linge, K. L. Trends in the solubility of iron, aluminium, manganese and phosphorus in aerosol collected over the Atlantic Ocean. *Mar Chem.* **2006**, *98* (1), 43–58.
- (9) Moore, C. M.; Mills, M. M.; Arrigo, K. R.; Berman-Frank, I.; Bopp, L.; Boyd, P. W.; Galbraith, E. D.; Geider, R. J.; Guieu, C.; Jaccard, S. L.; et al. Processes and patterns of oceanic nutrient limitation. *Nat. Geosci* **2013**, *6* (9), 701–710.
- (10) Trommer, G.; Leynaert, A.; Klein, C.; Naegelen, A.; Beker, B. Phytoplankton phosphorus limitation in a North Atlantic coastal ecosystem not predicted by nutrient load. *J. Plankton Res.* **2013**, 35 (6), 1207–1219.
- (11) Arrigo, K. R. Marine microorganisms and global nutrient cycles (vol 437, pg 349, 2005). *Nature* **2005**, 438 (7064), 122–122.
- (12) Wang, R.; Balkanski, Y.; Boucher, O.; Ciais, P.; Peñuelas, J.; Tao, S. Significant contribution of combustion-related emissions to the atmospheric phosphorus budget. *Nat. Geosci* **2015**, 8 (1), 48–54.
- (13) Mahowald, N. M.; Artaxo, P.; Baker, A. R.; Jickells, T. D.; Okin, G. S.; Randerson, J. T.; Townsend, A. R. Impacts of biomass burning emissions and land use change on Amazonian atmospheric phosphorus cycling and deposition. *Global Biogeochem Cy* **2005**, *19* (4), No. Gb4030.

- (14) Tipping, E.; Benham, S.; Boyle, J. F.; Crow, P.; Davies, J.; Fischer, U.; Guyatt, H.; Helliwell, R.; Jackson-Blake, L.; Lawlor, A. J.; et al. Atmospheric deposition of phosphorus to land and freshwater. *Environ. Sci-Proc. Imp* **2014**, *16* (7), 1608–1617.
- (15) Richards, S.; Marshall, R.; Lag-Brotons, A. J.; Semple, K. T.; Stutter, M. Phosphorus solubility changes following additions of bioenergy wastes to an agricultural soil: Implications for crop availability and environmental mobility. *Geoderma* **2021**, *401*, No. 115150.
- (16) Ni, J. Y.; Lin, P.; Zhen, Y.; Yao, X. Y.; Guo, L. D. Distribution, source and chemical speciation of phosphorus in surface sediments of the central Pacific Ocean. *Deep-Sea Res. Pt I* **2015**, *105*, 74–82.
- (17) Moore, C. M.; Mills, M. M.; Langlois, R.; Milne, A.; Achterberg, E. P.; La Roche, J.; Geider, R. J. Relative influence of nitrogen and phosphorus availability on phytoplankton physiology and productivity in the oligotrophic sub-tropical North Atlantic Ocean. *Limnol Oceanogr* **2008**, *53* (1), 291–305.
- (18) Compton, J.; Mallinson, D.; Glenn, C. R.; Filippelli, G.; Follmi, K.; Shields, G.; Zanin, Y. Variations in the Global Phosphoruscycle. In *Marine Authigenesis: From Global to Microbial*; Glenn, C. R., Prévôt-Lucas, L., Lucas, J., Eds.; SEPM Society for Sedimentary Geology, 2000; Vol. 66; p 0.
- (19) Delaney, M. L. Phosphorus accumulation in marine sediments and the oceanic phosphorus cycle. *Global Biogeochem Cy* **1998**, *12* (4), 563–572.
- (20) Mills, M. M.; Moore, C. M.; Langlois, R.; Milne, A.; Achterberg, E.; Nachtigall, K.; Lochte, K.; Geider, R. J.; La Roche, J. Nitrogen and phosphorus co-limitation of bacterial productivity and growth in the oligotrophic subtropical North Atlantic. *Limnol. Oceanogr* **2008**, 53 (2), 824–834.
- (21) Christodoulaki, S.; Petihakis, G.; Kanakidou, M.; Mihalopoulos, N.; Tsiaras, K.; Triantafyllou, G. Atmospheric deposition in the Eastern Mediterranean. A driving force for ecosystem dynamics. *J. Marine Syst* **2013**, *109*, 78–93.
- (22) Richon, C.; Dutay, J. C.; Dulac, F.; Wang, R.; Balkanski, Y. Modeling the biogeochemical impact of atmospheric phosphate deposition from desert dust and combustion sources to the Mediterranean Sea. *Biogeosciences* **2018**, *15* (8), 2499–2524.
- (23) Herbert, R. J.; Krom, M. D.; Carslaw, K. S.; Stockdale, A.; Mortimer, R. J. G.; Benning, L. G.; Pringle, K.; Browse, J. The Effect of Atmospheric Acid Processing on the Global Deposition of Bioavailable Phosphorus From Dust. *Global Biogeochem Cy* **2018**, 32 (9), 1367–1385.
- (24) Berthold, M.; Wulff, R.; Reiff, V.; Karsten, U.; Nausch, G.; Schumann, R. Magnitude and influence of atmospheric phosphorus deposition on the southern Baltic Sea coast over 23years: implications for coastal waters. *Environ. Sci. Eur.* **2019**, *31*, 27.
- (25) Reynolds, C. S.; Davies, P. S. Sources and bioavailability of phosphorus fractions in freshwaters: a British perspective. *Biol. Rev.* **2001**, 76 (1), 27–64.
- (26) Vet, R.; Artz, R. S.; Carou, S.; Shaw, M.; Ro, C. U.; Aas, W.; Baker, A.; Bowersox, V. C.; Dentener, F.; Galy-Lacaux, C.; et al. A global assessment of precipitation chemistry and deposition of sulfur, nitrogen, sea salt, base cations, organic acids, acidity and pH, and phosphorus. *Atmos. Environ.* **2014**, 93, 3–100.
- (27) Meng, Y.; Li, R.; Fu, H. B.; Bing, H. J.; Huang, K.; Wu, Y. H. The Sources and Atmospheric Pathway of Phosphorus to a High Alpine Forest in Eastern Tibetan Plateau, China. *J. Geophys Res-Atmos* **2020**, *125* (4), No. e2019JD031327.
- (28) Myriokefalitakis, S.; Nenes, A.; Baker, A. R.; Mihalopoulos, N.; Kanakidou, M. Bioavailable atmospheric phosphorous supply to the global ocean: a 3-D global modeling study. *Biogeosciences* **2016**, *13* (24), 6519–6543.
- (29) Okin, G. S.; Baker, A. R.; Tegen, I.; Mahowald, N. M.; Dentener, F. J.; Duce, R. A.; Galloway, J. N.; Hunter, K.; Kanakidou, M.; Kubilay, N.; Prospero, J. M.; Sarin, M.; Surapipith, V.; Uematsu, M.; Zhu, T. Impacts of atmospheric nutrient deposition on marine productivity: Roles of nitrogen, phosphorus, and iron. *Global Biogeochem. Cycles* **2011**, 25, No. Gb2022.

- (30) Nenes, A.; Krom, M. D.; Mihalopoulos, N.; Van Cappellen, P.; Shi, Z.; Bougiatioti, A.; Zarmpas, P.; Herut, B. Atmospheric acidification of mineral aerosols: a source of bioavailable phosphorus for the oceans. *Atmos Chem. Phys.* **2011**, *11* (13), 6265–6272.
- (31) Baker, A. R.; Kanakidou, M.; Nenes, A.; Myriokefalitakis, S.; Croot, P. L.; Duce, R. A.; Gao, Y.; Guieu, C.; Ito, A.; Jickells, T. D.; et al. Changing atmospheric acidity as a modulator of nutrient deposition and ocean biogeochemistry. *Sci. Adv.* **2021**, *7* (28), No. eabd8800.
- (32) Stockdale, A.; Krom, M. D.; Mortimer, R. J. G.; Benning, L. G.; Carslaw, K. S.; Herbert, R. J.; Shi, Z. B.; Myriokefalitakis, S.; Kanakidou, M.; Nenes, A. Understanding the nature of atmospheric acid processing of mineral dusts in supplying bioavailable phosphorus to the oceans. *P Natl. Acad. Sci. USA* **2016**, *113* (51), 14639–14644.
- (33) Zamora, L. M.; Prospero, J. M.; Hansell, D. A.; Trapp, J. M. Atmospheric P deposition to the subtropical North Atlantic: sources, properties, and relationship to N deposition. *J. Geophys Res-Atmos* **2013**, *118* (3), 1546–1562.
- (34) Baker, A. R.; Jickells, T. D.; Biswas, K. F.; Weston, K.; French, M. Nutrients in atmospheric aerosol particles along the Atlantic Meridional Transect. *Deep-Sea Res. Pt Ii* **2006**, 53 (14–16), 1706–1719.
- (35) Fomba, K. W.; Deabji, N.; Barcha, S. E.; Ouchen, I.; Elbaramoussi, E.; El Moursli, R. C.; Harnafi, M.; El Hajjaji, S.; Mellouki, A.; Herrmann, H. Application of TXRF in monitoring trace metals in particulate matter and cloud water. *Atmos Meas Tech* **2020**, 13 (9), 4773–4790.
- (36) Chen, H. Y.; Fang, T. H.; Preston, M. R.; Lin, S. Characterization of phosphorus in the aerosol of a coastal atmosphere: Using a sequential extraction method. *Atmos. Environ.* **2006**, *40* (2), 279–289.
- (37) Aspila, K. I.; Agemian, H.; Chau, A. S. Y. Semiautomated Method for Determination of Inorganic, Organic and Total Phosphate in Sediments. *Analyst* **1976**, *101* (1200), 187–197.
- (38) Murphy, J.; Riley, J. P. A modified single solution method for the determination of phosphate in natural waters. *Anal. Chim. Acta* **1962**, *27*, 31–36.
- (39) Deabji, N.; Fomba, K. W.; El Hajjaji, S.; Mellouki, A.; Poulain, L.; Zeppenfeld, S.; Herrmann, H. First insights into northern Africa high-altitude background aerosol chemical composition and source influences. *Atmos Chem. Phys.* **2021**, *21* (24), 18147–18174.
- (40) Iinuma, Y.; Engling, G.; Puxbaum, H.; Herrmann, H. A highly resolved anion-exchange chromatographic method for determination of saccharidic tracers for biomass combustion and primary bioparticles in atmospheric aerosol. *Atmos. Environ.* **2009**, *43* (6), 1367–1371.
- (41) Stein, A. F.; Draxler, R. R.; Rolph, G. D.; Stunder, B. J. B.; Cohen, M. D.; Ngan, F. Noaa's Hysplit Atmospheric Transport and Dispersion Modeling System. *B Am. Meteorol Soc.* **2015**, *96* (12), 2059–2077.
- (42) Mace, A.; Sommariva, R.; Fleming, Z.; Wang, W. Adaptive K-Means for Clustering Air Mass Trajectories. In *Intelligent Data Engineering and Automated Learning IDEAL 2011*; Yin, H., Wang, W., Rayward-Smith, V.,, Eds.; Springer: Berlin, 2011; pp 1–8.
- (43) Abdalmogith, S. S.; Harrison, R. M. The use of trajectory cluster analysis to examine the long-range transport of secondary inorganic aerosol in the UK. *Atmos. Environ.* **2005**, *39* (35), 6686–6695.
- (44) Bycenkiene, S.; Dudoitis, V.; Ulevicius, V. The Use of Trajectory Cluster Analysis to Evaluate the Long-Range Transport of Black Carbon Aerosol in the South-Eastern Baltic Region. *Adv. Meteorol.* **2014**, 2014, No. 137694.
- (45) Carslaw, D. C.; Ropkins, K. openair An R package for air quality data analysis. *Environ. Modell Softw* **2012**, 27–28, 52–61.
- (46) van Pinxteren, D.; Mothes, F.; Spindler, G.; Fomba, K. W.; Herrmann, H. Trans-boundary PM10: Quantifying impact and sources during winter 2016/17 in eastern Germany. *Atmos. Environ.* **2019**, 200, 119–130.

- (47) Fomba, K. W.; Faboya, O. L.; Deabji, N.; Makhmudov, A.; Hofer, J.; Souza, E. J. D.; Müller, K.; Althausen, D.; Sharipov, S.; Abdullaev, S.; et al. The seasonal variation of Asian dust, anthropogenic PM, and their sources in Dushanbe, Tajikistan. *Atmos. Environ.* **2024**, 333, No. 120667.
- (48) Nyanganyura, D.; Maenhaut, W.; Mathuthu, M.; Makarau, A.; Meixner, F. X. The chemical composition of tropospheric aerosols and their contributing sources to a continental background site in northern Zimbabwe from 1994 to 2000. *Atmos. Environ.* **2007**, *41* (12), 2644–2659.
- (49) Klopper, D.; Formenti, P.; Namwoonde, A.; Cazaunau, M.; Chevaillier, S.; Feron, A.; Gaimoz, C.; Hease, P.; Lahmidi, F.; Mirande-Bret, C.; et al. Chemical composition and source apportionment of atmospheric aerosols on the Namibian coast. *Atmos Chem. Phys.* **2020**, 20 (24), 15811–15833.
- (50) Artaxo, P.; Martins, J. V.; Yamasoe, M. A.; Procópio, A. S.; Pauliquevis, T. M.; Andreae, M. O.; Guyon, P.; Gatti, L. V.; Leal, A. M. C. Physical and chemical properties of aerosols in the wet and dry seasons in Rondonia, Amazonia -: art. no. 8081. *J. Geophys Res-Atmos* **2002**, *107* (D20), 8081.
- (51) Hsu, S. C.; Gong, G. C.; Shiah, F. K.; Hung, C. C.; Kao, S. J.; Zhang, R.; Chen, W. N.; Chen, C. C.; Chou, C. C. K.; Lin, Y. C.; et al. Sources, solubility, and acid processing of aerosol iron and phosphorous over the South China Sea: East Asian dust and pollution outflows vs. Southeast Asian biomass burning. *Atmos. Chem. Phys. Discuss.* **2014**, 2014, 21433–21472.
- (52) Sun, C. X.; Z, Q.; Kang, H.; Yu, J. Phosphorus in the aerosols over oceans transported offshore from China to the Arctic Ocean: Speciation, spatial distribution, and potential sources. *Adv. Polar. Sci.* **2015**, *26*, 232–238.
- (53) Izquierdo, R.; Benítez-Nelson, C. R.; Masqué, P.; Castillo, S.; Alastuey, A.; Avila, A. Atmospheric phosphorus deposition in a near-coastal rural site in the NE Iberian Peninsula and its role in marine productivity. *Atmos. Environ.* **2012**, *49*, 361–370.
- (54) Shi, J. H.; Wang, N.; Gao, H. W.; Baker, A. R.; Yao, X. H.; Zhang, D. Z. Phosphorus solubility in aerosol particles related to particle sources and atmospheric acidification in Asian continental outflow. *Atmos Chem. Phys.* **2019**, *19* (2), 847–860.
- (55) Barkley, A. E.; Prospero, J. M.; Mahowald, N.; Hamilton, D. S.; Popendorf, K. J.; Oehlert, A. M.; Pourmand, A.; Gatineau, A.; Panechou-Pulcherie, K.; Blackwelder, P.; et al. African biomass burning is a substantial source of phosphorus deposition to the Amazon, Tropical Atlantic Ocean, and Southern Ocean. *P Natl. Acad. Sci. USA* 2019, 116 (33), 16216–16221.
- (56) Adesina, J. A.; Piketh, S. J.; Formenti, P.; Maggs-Kölling, G.; Holben, B. N.; Sorokin, M. G. Aerosol optical properties and direct radiative effect over Gobabeb, Namibia. *Clean Air J.* **2019**, 29 (2). DOI: 10.17159/caj/2019/29/2.7518.
- (57) Schepanski, K.; Tegen, I.; Macke, A. Saharan dust transport and deposition towards the tropical northern Atlantic. *Atmos Chem. Phys.* **2009**, 9 (4), 1173–1189.
- (58) Fomba, K. W.; Müller, K.; van Pinxteren, D.; Poulain, L.; van Pinxteren, M.; Herrmann, H. Long-term chemical characterization of tropical and marine aerosols at the Cape Verde Atmospheric Observatory (CVAO) from 2007 to 2011. *Atmos Chem. Phys.* **2014**, 14 (17), 8883–8904.
- (59) Chen, Y.; Mills, S.; Street, J.; Golan, D.; Post, A.; Jacobson, M.; Paytan, A. Estimates of atmospheric dry deposition and associated input of nutrients to Gulf of Aqaba seawater. *J. Geophys Res-Atmos* **2007**, *112* (D4), No. D04309.
- (60) Fomba, K. W.; Muller, K.; van Pinxteren, D.; Herrmann, H. Aerosol size-resolved trace metal composition in remote northern tropical Atlantic marine environment: case study Cape Verde islands. *Atmos Chem. Phys.* **2013**, *13* (9), 4801–4814.
- (61) Sholkovitz, E. R.; Sedwick, P. N.; Church, T. M.; Baker, A. R.; Powell, C. F. Fractional solubility of aerosol iron: Synthesis of a global-scale data set. *Geochim Cosmochim Ac* **2012**, *89*, 173–189.
- (62) Zhang, H. H.; Li, R.; Dong, S. W.; Wang, F.; Zhu, Y. J.; Meng, H.; Huang, C. P.; Ren, Y.; Wang, X. F.; Hu, X. D.; et al. Abundance

- and Fractional Solubility of Aerosol Iron During Winter at a Coastal City in Northern China: Similarities and Contrasts Between Fine and Coarse Particles. *J. Geophys Res-Atmos* **2022**, *127* (1), No. e2021[D036070.
- (63) Jin, X. M.; Zhu, Q. D.; Cohen, R. C. Direct estimates of biomass burning NOx emissions and lifetimes using daily observations from TROPOMI. *Atmos Chem. Phys.* **2021**, *21* (20), 15569–15587.
- (64) Tilgner, A.; Schaefer, T.; Alexander, B.; Barth, M.; Collett, J. L.; Fahey, K. M.; Nenes, A.; Pye, H. O. T.; Herrmann, H.; McNeill, V. F. Acidity and the multiphase chemistry of atmospheric aqueous particles and clouds. *Atmos Chem. Phys.* **2021**, *21* (17), 13483–13536.
- (65) Li, T.; Wang, Z.; Wang, Y. R.; Wu, C.; Liang, Y. H.; Xia, M.; Yu, C.; Yun, H.; Wang, W. H.; Wang, Y.; et al. Chemical characteristics of cloud water and the impacts on aerosol properties at a subtropical mountain site in Hong Kong SAR. *Atmos Chem. Phys.* **2020**, 20 (1), 391–407.
- (66) Pye, H. O. T.; Ward-Caviness, C. K.; Murphy, B. N.; Appel, K. W.; Seltzer, K. M. Secondary organic aerosol association with cardiorespiratory disease mortality in the United States. *Nat. Commun.* **2021**, *12* (1), 7215.
- (67) Andersen, H.; Cermak, J.; Solodovnik, I.; Lelli, L.; Vogt, R. Spatiotemporal dynamics of fog and low clouds in the Namib unveiled with ground- and space-based observations. *Atmos Chem. Phys.* **2019**, *19* (7), 4383–4392.
- (68) Mahowald, N.; Jickells, T. D.; Baker, A. R.; Artaxo, P.; Benitez-Nelson, C. R.; Bergametti, G.; Bond, T. C.; Chen, Y.; Cohen, D. D.; Herut, B.; et al. Global distribution of atmospheric phosphorus sources, concentrations and deposition rates, and anthropogenic impacts. *Global Biogeochem Cy* **2008**, 22 (4), No. Gb4026.
- (69) Herut, B.; Collier, R.; Krom, M. D. The role of dust in supplying nitrogen and phosphorus to the Southeast Mediterranean. *Limnol Oceanogr* **2002**, *47* (3), 870–878.
- (70) Anderson, L. D.; Faul, K. L.; Paytan, A. Phosphorus associations in aerosols: What can they tell us about P bioavailability? *Mar Chem.* **2010**, *120* (1–4), 44–56.
- (71) Mims, S. A.; Mims, F. M. Fungal spores are transported long distances in smoke from biomass fires. *Atmos. Environ.* **2004**, 38 (5), 651–655.
- (72) van Pinxteren, M.; Fomba, K. W.; Triesch, N.; Stolle, C.; Wurl, O.; Bahlmann, E.; Gong, X. D.; Voigtländer, J.; Wex, H.; Robinson, T. B.; et al. Marine organic matter in the remote environment of the Cape Verde islands an introduction and overview to the MarParCloud campaign. *Atmos Chem. Phys.* **2020**, 20 (11), 6921–6951.
- (73) Mine, A. H.; Coleman, M. L.; Colman, A. S. Phosphorus Release and Regeneration Following Laboratory Lysis of Bacterial Cells. *Front Microbiol* **2021**, *12*, No. 641700.
- (74) Fu, W. Y.; Zhang, X. H. Global phosphorus dynamics in terms of phosphine. *Npj Clim Atmos Sci.* **2020**, 3 (1), 51.
- (75) García, M. I.; van Drooge, B. L.; Rodríguez, S.; Alastuey, A. Speciation of organic aerosols in the Saharan Air Layer and in the free troposphere westerlies. *Atmos Chem. Phys.* **2017**, *17* (14), 8939–8958.
- (76) Belnap, J. The world at your feet: desert biological soil crusts. Front Ecol Environ 2003, 1 (4), 181–189.
- (77) Desboeufs, K.; Formenti, P.; Torres-Sánchez, R.; Schepanski, K.; Chaboureau, J. P.; Andersen, H.; Cermak, J.; Feuerstein, S.; Laurent, B.; Klopper, D.; et al. Fractional solubility of iron in mineral dust aerosols over coastal Namibia: a link to marine biogenic emissions? *Atmos Chem. Phys.* **2024**, *24* (2), 1525–1541.
- (78) Dam, T. T. N.; Angert, A.; Krom, M. D.; Bigio, L.; Hu, Y. F.; Beyer, K. A.; Mayol-Bracero, O. L.; Santos-Figueroa, G.; Pio, C.; Zhu, M. Q. X-ray Spectroscopic Quantification of Phosphorus Transformation in Saharan Dust during Trans-Atlantic Dust Transport. *Environ. Sci. Technol.* **2021**, *55* (18), 12694–12703.
- (79) Spokes, L.; Jickells, T.; Jarvis, K. Atmospheric inputs of trace metals to the northeast Atlantic Ocean: the importance of southeasterly flow. *Mar Chem.* **2001**, *76* (4), 319–330.
- (80) Kocak, M.; Mihalopoulos, N.; Tutsak, E.; Violaki, K.; Theodosi, C.; Zarmpas, P.; Kalegeri, P. Atmospheric Deposition of Macro-

- nutrients (Dissolved Inorganic Nitrogen and Phosphorous) onto the Black Sea and Implications on Marine Productivity\*. *J. Atmos Sci.* **2016**, 73 (4), 1727–1739.
- (81) Zamora, L. M.; Landolfi, A.; Oschlies, A.; Hansell, D. A.; Dietze, H.; Dentener, F. Atmospheric deposition of nutrients and excess N formation in the North Atlantic. *Biogeosciences* **2010**, *7* (2), 777–793
- (82) Markaki, Z.; Oikonomou, K.; Kocak, M.; Kouvarakis, G.; Chaniotaki, A.; Kubilay, N.; Mihalopoulos, N. Atmospheric deposition of inorganic phosphorus in the Levantine Basin, eastern Mediterranean: Spatial and temporal variability and its role in seawater productivity. *Limnology and Oceanography* **2003**, 48 (4), 1557–1568.
- (83) Srinivas, B.; Sarin, M. M. Atmospheric pathways of phosphorous to the Bay of Bengal: contribution from anthropogenic sources and mineral dust. *Tellus B* **2022**, *64*, 17174.
- (84) Browning, T. J.; Achterberg, E. P.; Rapp, I.; Engel, A.; Bertrand, E. M.; Tagliabue, A.; Moore, C. M. Nutrient co-limitation at the boundary of an oceanic gyre. *Nature* **2017**, *551* (7679), 242–246.
- (85) Mills, M. M.; Ridame, C.; Davey, M.; La Roche, J.; Geider, R. J. Iron and phosphorus co-limit nitrogen fixation in the eastern tropical North Atlantic. *Nature* **2004**, *429* (6989), 292–294.
- (86) Moore, C. M.; Mills, M. M.; Achterberg, E. P.; Geider, R. J.; LaRoche, J.; Lucas, M. I.; McDonagh, E. L.; Pan, X.; Poulton, A. J.; Rijkenberg, M. J. A.; et al. Large-scale distribution of Atlantic nitrogen fixation controlled by iron availability. *Nat. Geosci.* **2009**, 2 (12), 867–871.
- (87) Jin, H. Y.; Zhang, C.; Meng, S. Y.; Wang, Q.; Ding, X. K.; Meng, L.; Zhuang, Y. Y.; Yao, X. H.; Gao, Y.; Shi, F.; et al. Atmospheric deposition and river runoff stimulate the utilization of dissolved organic phosphorus in coastal seas. *Nat. Commun.* **2024**, *15* (1), 658.
- (88) Rijkenberg, M. J. A.; Langlois, R. J.; Mills, M. M.; Patey, M. D.; Hill, P. G.; Nielsdóttir, M. C.; Compton, T. J.; LaRoche, J.; Achterberg, E. P. Environmental Forcing of Nitrogen Fixation in the Eastern Tropical and Sub-Tropical North Atlantic Ocean. *PLoS One* **2011**, *6* (12), No. e28989.
- (89) Guignard, M. S.; Leitch, A. R.; Acquisti, C.; Eizaguirre, C.; Elser, J. J.; Hessen, D. O.; Jeyasingh, P. D.; Neiman, M.; Richardson, A. E.; Soltis, P. S.; et al. Impacts of Nitrogen and Phosphorus: From Genomes to Natural Ecosystems and Agriculture. *Front Ecol Evol* **2017**, *5*, 70.
- (90) Luo, X.; Mazer, S. J.; Guo, H.; Zhang, N.; Weiner, J.; Hu, S. J. Nitrogen: phosphorous supply ratio and allometry in five alpine plant species. *Ecol Evol* **2016**, *6* (24), 8881–8892.